DOI: https://doi.org/10.55981/mipi.2023.1665
E- ISSN 2541-1233

Majalah Ilmiah Pengkajian Industri
(Journal of Industrial Research and Innovation)

Vol.17, No 02, September 2023 - (33-40)

Journal homepage: https://ejurnal.brin.go.id/MIPI

Crashworthiness Analysis of the Impact Modules of Indonesian High-Speed Train Considering EN 15227

Yohanes Pringeten Dilianto Sembiring Depari [1, 2], Achmad Syaifudin[1,*], Yunendar Aryo Handoko[3], Adhi Dharma Permana[2], Hendrato[2], Beny Halfina[2], Jean Mario Valentino[2]

[1]*Institut Teknologi Sepuluh November (ITS), Indonesia*
[2]*National Research and Innovation Agency (BRIN), Indonesia*
[3]*Institut Teknologi Bandung (ITB), Indonesia*

*Correspondence email: saifudin@me.its.ac.id

ABSTRACT

A crashworthiness structure is being developed for the passive safety system of the Indonesian High-speed Train design. It is made up of an anti-climber, a crash buffer, and a honeycomb in sequential arrangement. The issue addressed in this research is the need for thorough verification of the design of impact modules and the supporting frame for compliance with the EN 15227 standard. The finite element method approach is used to analyze the feasibility of a collision in a high-speed train's passive safety system. The geometry of the finite element model is constructed as a surface element and refers to the model designed by the National Research and Innovation Agency (BRIN) and the Indonesian Railways Company (PT. INKA). In accordance with the train design plan, aluminum 6005A-T6 is implemented. Simulations were conducted at initial velocities of 10 m/s using the LS-DYNA solver. The time interval during which the velocity changes is considered the time when the kinetic energy of the collision is completely absorbed. The simulation results indicate that the kinetic energy can be effectively absorbed by the crash module and the mask-of-car frame, as long as the initial contact between the trains occurs at the anti-climber. The impact kinetic energy stored in the crash buffer system is 63%, equivalent to 959 kJ, while the remaining 37%, amounting to 561 kJ, is absorbed by the cab and honeycomb frame structure. Thus, the crash structure being developed complies with the crashworthiness standard.

ARTICLE INFO

Article History:

Received	*02 April 2023*
1st Revision	*22 June 2023*
2nd Revision	*23 August 2023*
Accepted	*08 September 2023*
Available Online	*29 September 2023*

Keyword:
Crashworthiness;
EN15227;
High-Speed Train;
Mask of Car;
Passive Safety

***Corresponding Author | Achmad Syaifudin|✉ saifudin@me.its.ac.id**

INTRODUCTION

The Government of Indonesia started the High-Speed Train (HST) project to modernize public transportation to promote connection and mobility between cities. To support this purpose, the National Research and Innovation Agency (Badan Riset dan Inovasi Nasional, BRIN) has begun building a prototype high-speed railway with a maximum top speed of 250 km/h. At greater speeds, train safety has become a significant issue, particularly in terms of the crashworthiness of the structure [1][2].

Railway structures must be designed to reduce the risk of passenger fatalities in an accident. Structure crashworthiness is characterized as a structure's ability to maintain passengers' safety in the case of an accident. One factor for lowering the danger to passengers in case of an accident is the strength of the primary structure. This avoids excessive plastic deformation of the primary structure that might directly compromise passenger safety. Crashworthiness energy-absorbing structures are crucial safety standards for the transportation and aerospace industries. Those energy-absorbing structures need to absorb enormous quantities of kinetic energy in a controlled and consistent way to protect occupants and passengers from catastrophic harm in the event of a collision [3]. There are various techniques to increase crash safety, mostly linked to choosing materials and design structures [4][5][6].

Several collision safety analyses have been done to increase the safety of the structure train [7]. Egger et al. explored more demanding crash safety criteria and produced lightweight constructions to achieve them [8]. Lewis et al. studied IC255 train-vehicle collisions in detail[9]. Walter analyzed the new European criteria for the safety of the train and their influence on train safety [10]. Jacobsen et al. performed numerous experiments on rail passengers to demonstrate a certain level of improvement in performance from different design options for passenger locomotive crash safety [11]. Railway-highway crash calculations following scenario three based on EN 15227, examining the construction of deformable barriers [12]. Carolan et al. assessed the efficacy of a particular crash energy management system (CEM) design for a passenger railway [13]. The objective was to discover component modifications that might increase passenger vehicle crashworthiness beyond the basic CEM design without harming the occupants. ONeill and Carruthers presented a railway that performs the level intersection impact criteria stated in European collision safety regulations, according to the initial concept design and assessment of lightweight energy-absorbing structures for transportation [14]. Tyrell et al. developed six experiments to assess the collision safety of current devices and the efficiency of systems with CEM features [15]. The crash scenario studied in these trials was a collision between a front-cabin passenger train and a traditional locomotive train. Zangani et al. accomplished test investigations and used finite element analysis to predict the performance of aluminum joins in railway wagons throughout extremely dynamic load requirements, giving guidance for development to limit the potential of weld cracks [16]; Xue and Schmid investigated the incident involving the safety of traditional designed railway trains for passengers and proposed improvements for development [17]. Witkowski et al. proved topological performance [18], whereas Chuang and Yang reviewed three commercially accessible optimizations of topology approaches for crash-safety development [19].

The crashworthiness structure of the transportation greatly affects its collision obstruction. In addition to material selections and loading methods, the energy absorption of crashworthiness structures mostly relies on morphological characteristics like the cross-section area and volume. Hence, finding adequate structural characteristics to maximize vehicle crashworthiness through optimum design is a critical problem for the passive safety protection of railway vehicles [1]. The deformation occurring in the vehicle structure during impact loads is nonlinear. As a result, comprehensive calculations for target functions, including characteristic variables for energy absorption in the structure, cannot be generated by modifying the structural parameters. Consequently, many experiments must be accomplished to determine the appropriate settings utilizing the trial-and-error approach. However, this approach is expensive and needs to ensure that the generated parameter combinations are optimal. Therefore, specific modeling optimization methodologies must be utilized to optimize the crashworthiness design of buildings.

Structural crashworthiness studies and investigations delve into assessing a structure's response to dynamic loads, often involving significant impacts, to mitigate their effects and enhance the performance of suboptimal structures. This is undertaken to minimize the impact and collision's forces repercussions. The objective is to increase crash safety by managing impact energy during collisions and refining the energy management of the involved structures. Efforts to handle impact energy from instantaneous dynamic loading have been pursued through two structural design approaches: integrated absorbent structures and dedicated energy-absorbing structures. Research on integrated energy-absorbing structures aims to improve the effectiveness of passive safety technologies. Research on specialized energy-absorbing structures seeks to create designs that effectively absorb collision and impact energy without transmitting damage or dissipation to other interconnected structures [20].

The issue addressed in this research is the need for a thorough verification of the design of impact modules and the supporting frame for compliance with the EN 15227 standard [21]. The model employed for this study is based on the geometry and structure of an Indonesian express train developed in collaboration between BRIN and PT INKA. The conclusions of this research are intended to serve as a benchmark to improve the crashworthiness of high-speed trains, especially in terms of the main body's ability to absorb the remaining impact energy. These findings may apply to prospective high-speed rail projects, complying with national and international standards.

METHODS

This research employs the model developed by BRIN and INKA. Models were designed using Autodesk Inventor 2022. The model contains an Anti-climber, crash buffer, honeycomb, and mask-of-car. In particular, the study will analyze the main frontal structure of the train, referred to as the mask-of-car, as depicted in **Figure 1**. The exterior shape of the mask-of-car was designed and optimized using aerodynamic simulation while accounting for the space needed for crashworthiness components [22]. The interior structure consists of various components, including the frame structure of the driver's cabin, the crash buffer, the anti-climbing device, and the honeycomb structure. This structure is designed to withstand forces during a frontal impact. Therefore, correct calculations are needed to guarantee the passengers and the machinist crew's assurance.

Table 1. Mechanical Property Aluminum 6005A-T6 [23]

Parameter	Value	Unit
Density (ρ)	2700	kg/m^3
Tensile Yield Strength	230	MPa
Tensile Ultimate Strength	280	Mpa
Poisson rasio (v)	0,3	-
Modulus elastisitas (E)	70	GPa
Initial Yield Stress (A)	270	MPa
Hardening Constant (B)	134	MPa
Strain Hardening Coefficient (n)	0,514	-
Strain Rate Constant (C)	0,0082	-
Thermal softening exponent (m)	0,703	-
Melting Temperature (TM)	893	K
Room Temperature (TR)	293	K
Reference Strain Rate (peso)	0,001	/Sec
Specific heat (cp)	910	J/kg. K
Failure Parameter 1 (D1)	0,06	-
Failure Parameter 2 (D2)	0,497	-
Failure Parameter 3 (D3)	-1,551	-
Failure Parameter 4 (D4)	0,0286	-
Failure Parameter 5 (D5)	6,8	-

The crashworthiness structure utilizes Al 6005A-T6 aluminum. The isotropic elastic material concept was employed to characterize the elastoplastic features of the material, and the Johnson-Cook strength concept was utilized to explicate the material response at high strain rates. The material property data for al 6005A-T6 were obtained from a numerical simulation of extruded panels conducted using LS-DYNA software, as described in **Table 1**. The failure of a material's properties is often categorized into fractured failure (fracture) or ductility (yield) failure. According to the factors (like the heat, condition of stress, and loading ratio), most substances may shatter in a ductile or brittle fashion or both [23].

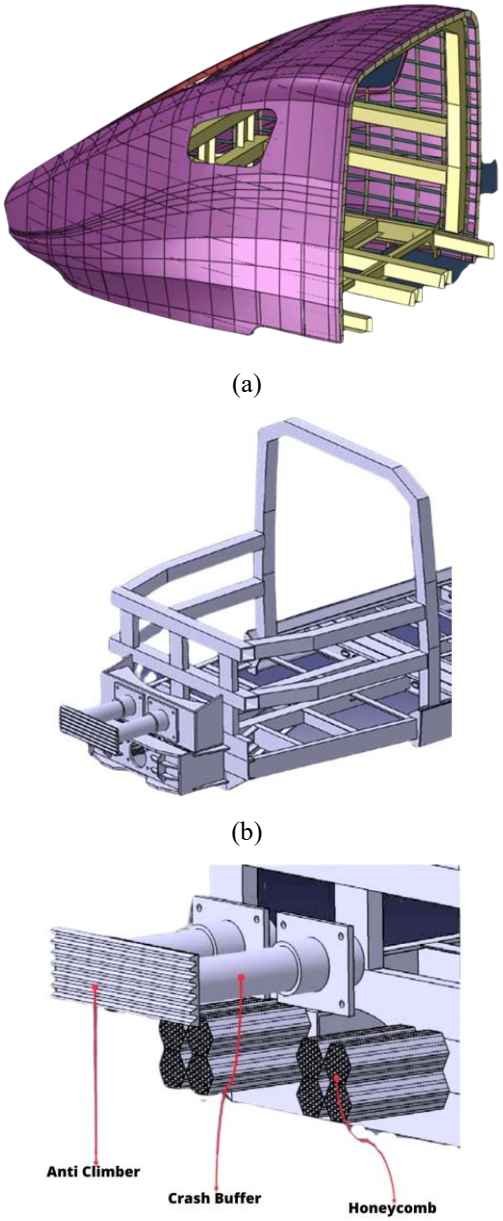

Figure 1. Drawing design of (a) Mask-of-car, (b) structure of crashworthiness mask of car (c) component of crashworthiness mask of car

The criteria used in the design of train crashworthiness structures are as follows.

a. Regulation No. 175 of the Ministry of Transport of 2015, Technical standards for trains, Article 13 c): Impact loads resulting from collisions. Resistance to shock loads resulting from collisions (crashworthiness) [24].
b. EN 15227:2008 [25] Collision safety standards for railway locomotive structures. These standards address minimum impact loads in terms of impact velocities. The standard specifies minimum impact loads based on impact velocities. It assumes that the front/rear structure of the train must be designed to absorb deformation and impact energy. To minimize the risk of passenger injury, the front/rear structure should be engineered to absorb and deform the impact energy, thus minimizing the potential for passenger harm.

To explicate the safety standard requirements for trains, PM 175 Article 13 c is fairly broad and depends on the interpretation of train crashworthiness using the EN 15227 standard. This standard includes circumstances relating to accidents that relied on specifications established by the International Union of Railways. The criteria include accident scenarios according to the International Union of Railways (UIC) standards. These are detailed in EN 15227:2008 in **Table 2**.

Table 2. Standard EN 15227:2008[25]

Category	Definition	Examples of vehicle types
C-1	Vehicles built to utilize Ten routes, worldwide, national, and regional networks (which involve level crossings).	Locomotives, coaches, and fixed train unit
C-2	Urban vehicles are supposed to run exclusively using appropriate railroad systems alongside highways.	Metro vehicles
C-3	Light rail vehicles are designed to run in urban and local networks, in track-sharing activities, and collaborate with highway traffic.	Tram train, peri-urban train
C-4	Light trains are designed to function on dedicated networks in cities interfacing with highways.	Tramway vehicle

High-speed train construction is classified as Category C-2, as are metro vehicles. This means that HST has dedicated lanes without intersections with other means of transport.

Table 3. Detail Standard Category II[25]

Design crash concept	Crash barrier	Operational features needed	Crash velocity *km/h* C-1	C-2	C-3	C-4
1	Similar railway unit	All Network	36	25	25	15
2	80-ton carriage	Combined traffic with cars fitted via side buffers	36	-	25	-
	129-ton regional train	Combined traffic with cars using a main coupler	-.	-	10	-
3	15-ton deformable obstacle	Ten and similar operations with level crossings	V-50 ≤ 100	-	25	-
	3-ton rigid obstacle	Urban lines avoiding segregation from road traffic	-	-	-	25
4	A small, low obstacle	Obstacle deflector requirements to be achieved		-		-

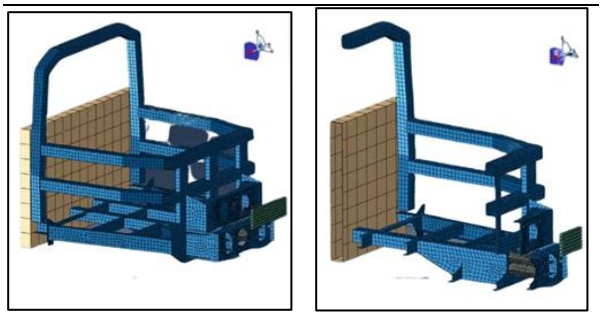

(a) (b)

Figure 2. Simulation Model for the Crashworthiness (a) Full Section, (b) Half Section

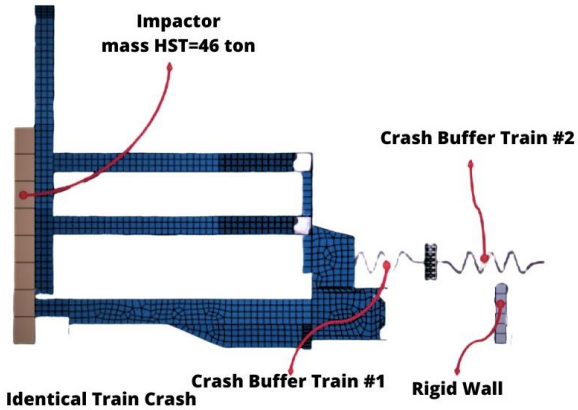

Figure 3. Test Setup for the Crash Safety Simulation

According to **Table 3**, the HST design can absorb impact loads at a 25 km/h crash speed using the same front-rear cable system crash scenario. To obtain more conservative crash analysis results, the decision was made to use a crash load scenario of 36 km/h with the same front-end rear system for simulating the crashworthiness of this high-speed train.

The crashworthiness study is accomplished by simulation utilizing numerical techniques or finite element approaches. The model of finite elements employed for the crashworthiness simulation is illustrated in. The structural design of HST crashworthiness is studied using EN 15227:2008 load scenarios at an impact velocity of 36 km/h (10 m/s).

The structure of the HST complies with the international standard EN 15227:2008. A scenario with maximum empty weight loading is assumed as it represents the most conservative impact velocity. The absorbed energy from impacts may be measured by determining the kinetic energy. The absorbed kinetic energy of the railway at the moment of collision may be measured as equation (1):

$$E_k = \frac{1}{2} m v^2 \quad (1)$$

Where m represents mass in kg, v stands for velocity in m/s, and Ek indicates the absorbed kinetic energy in kJ. The absorbed kinetic energy is 2,300 kJ when m is 46 tons and v is ten m/s. Furthermore, according to EN 15227:2008, in the case of a collision scenario with a similar train, the kinetic energy absorbed by both groups of trains is only half of the kinetic energy absorbed by each train. This implies that both trains exhibit comparable crash safety characteristics. The kinetic energy that the trains need to absorb is 1150 kJ. Since energy storage differs in meaning from energy absorption, the storage behavior is akin to the properties of a spring that can store energy for subsequent release. Therefore, in the high-speed train collision safety simulation, the crash buffers are represented as spring elements holding an energy storage capacity comparable to the crash buffers. Given that each train features two crash buffers, each train's cumulative energy storage capacity amounts to 1,520 kJ. The test setup for the crash safety simulation is illustrated in **Figure 3.**

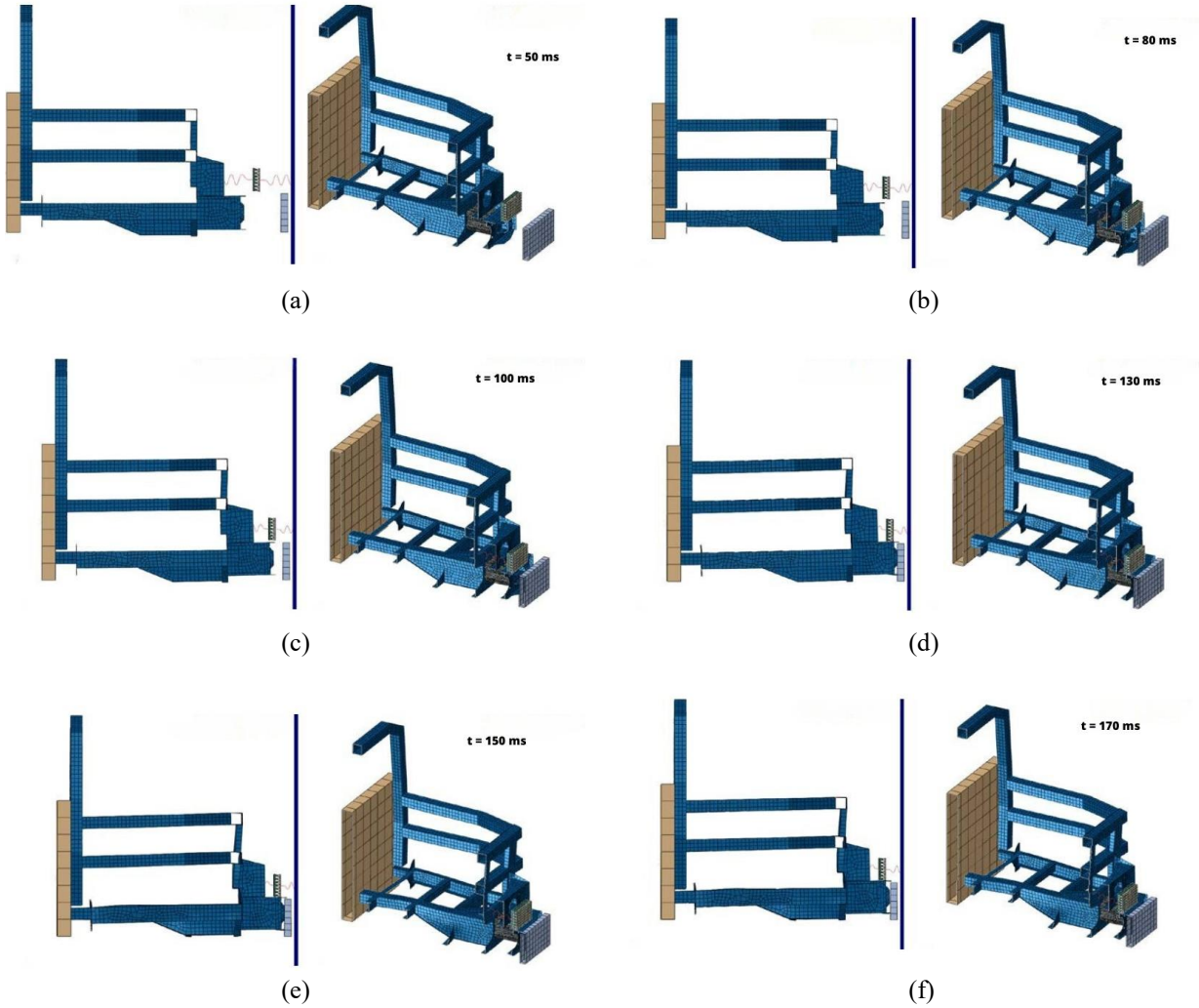

(a) (b) (c) (d) (e) (f)

Figure 4. Deformation of the Crashworthiness Frame in The Crash Scenario (a) t = 50 ms, (b) t = 80 ms, (c) t = 100 ms, (d) t = 130 ms, (e) t = 150 ms, (f) t = 170 ms

RESULTS AND DISCUSSION

During an impact, the CEM reacts in an orderly and coordinated way. The particular load passage follows a specified sequence across the collision zone, resulting in the progressive disintegration of the energy-absorbing elements. The connection device (coupler) manages the initial mobilizing component as envisioned. Under low forces, the buffer component of the connection device absorbs the force of impact energy. When the force approaches the buffer's constraint, normally roughly 1,000 kN, the connected device's collapsed tube becomes engaged, collecting energy until it is depleted [26]**.** Following that, the anti-climber absorbs a portion of the contact energy to prevent rollover. The impact loads are transferred to the primary energy absorber, which absorbs the largest portion of the impact energy. The CEM cab train can protect the driver by preserving a safety area and holding the cabin for passengers when the crumple area falls [27]. **Figure 4** shows the sequence of the crash structure's condition from 50 ms to 170 ms. Initially, the crash buffers of Train 1 and Train 2 were in contact, while the rigid wall was far from the crashworthiness structure. At this point, the load force has not yet been absorbed. Over the next 80 – 100 ms, the crash buffer takes the load in. The buffer crumples and the rigid wall approaches the main structure.

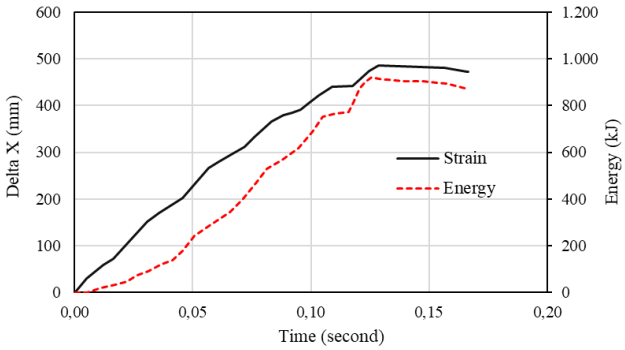

Figure 5. The deformation profile of the spring element and energy stored in the crash buffer

During 130 ms, the crash buffer reached its absorption limit, and the stiff wall finally made contact with the main structure. Following this contact with the main structure at 150 ms, the major structure starts absorbing the crash load. In the following 170 ms, the major structure begins to deform under the impact of the crash load. In the crashworthiness simulation for this crash scenario, the plastic deformation occurring in the main structure of the cabin frame is not significant since the initial contact between the trains happens at the anti-climber. It indicates that the bulk of the collision's kinetic energy is absorbed by the current crash safety structures, especially the crash buffer and the honeycomb structure. The cabin frame structure experiences a permanent displacement of -85.1 mm (shortened) along the X-axis (longitudinal) direction by the end of the impact.

That is a requirement for the quantity of impact energy that has to be handled by the crush area. That allows several alternatives for energy absorption. The most common option is to absorb 1 MJ during a crash. [25]. In this simulation, the total kinetic energy absorbed is 1,520 kJ. Of this, 959 kJ (63%) is stored in the train's accident buffer system. This is feasible due to the initial contact between the trains at the anti-climb point. In combination with the honeycomb, the mask-of-car frame absorbs the remaining 561 kJ (37%) of kinetic energy. This also fits with the stated EN 15227 standards [21]. **Figure 5** depicts the relationship between the change in length of the spring elements and the energy stored in the crash buffer system. Ideally, the honeycomb structure predominantly absorbs the remaining kinetic energy not stored in the crash cushioning material. As the primary structure, the honeycomb ideally absorbs most of the residual kinetic energy not stored in the crash cushioning material. This energy is absorbed through plastic deformation and gradually accumulates within the honeycomb [25].

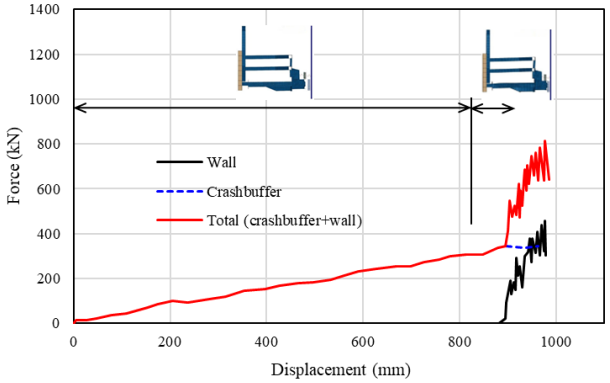

Figure 6. The Representative Plot Between Force and Displacement on the mask-of-car-frame

Figure 6 presents the representative plot between force and displacement on the mask-of-car frame. Assuming that the initial contact between the trains occurs at the anti-climber, it is evident that the energy is systematically stored in the crash buffer system until the trains contact the clutch housing. As mentioned in the preceding section, the crash buffer mechanism retains 63% of the impact energy. The mask-of-car frame and the honeycomb absorb 37% of the impact energy. This energy absorption process commences when the clutch housings come into contact and is marked by escalating impact forces on the rigid walls. The 37% of the impact energy absorbed by the frame and honeycomb material transpires at relatively short displacements, approximately 85 mm, and features significant peak forces of about 4,000 kN. This indicates that the crash box system is ineffective in absorbing the remaining kinetic energy. This might be attributed to the fact that the coupler enclosure structure, which serves as

the support (honeycomb) of the crash box, does not effectively transmit the impact forces to the honeycomb material, causing some of the impact forces to be transferred to the rear of the frame structure. This observation is apparent from the plastic stress level generated, as shown in **Figure 7**. Crash safety analyses reveal that, according to the UIC/EN 15227 standard, the crash bumper can notably absorb kinetic energy and the driver's seat frame structure, provided the initial contact between the trains occurs at the anti-climber.

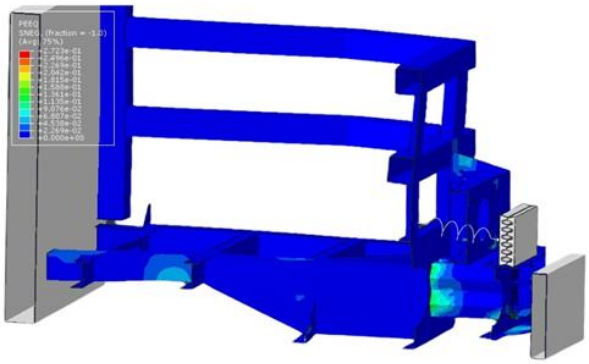

Figure 7. Plastic Strain of the Frame Component

CONCLUSION

The simulation indicates that the impact sequence began from the anti climber followed by the crash buffer and finally the honeycomb. The results reveal that the crash energy did not affect the passenger survival space during the impact. The crash buffer has the most deformations and absorbs all the remaining energy. In a collision scenario involving the same train at a speed of 36 km/h (10 m/s), the kinetic energy to be absorbed according to EN 15227 standard is 1,150 kJ. In collision scenarios without a coupler, since the initial contact between the trains takes place at the anti-climb bars, the collision energy is completely absorbed by the crashworthiness components of the HST car body structure. The study determined that 63%, or 959 kJ, of the resultant crash kinetic energy can be stored in the crash buffer system, while the remaining 37%, or 561 kJ, is absorbed by the mask of the car frame structure and honeycombs. The plastic deformation observed was 85 mm at a peak load of 4,000 kN. The crashworthiness analysis observed that, according to the UIC/EN 15227 standard, the kinetic energy was effectively absorbed by the crash buffer and the mask of the car frame structure, with the initial contact between the trains occurring at the anti-climb. The suggestions derived from this study propose that crash scenarios for the HST car body structure need to be studied with the first contact between the trains occurring at the coupler.

AUTHOR CONTRIBUTIONS

First Author, Second Author, and Third Author have contributed equally to this work.

ACKNOWLEDGEMENT

Indonesia National Research and Innovation Agency (BRIN) gave this study funds and Ansys Mechanical software. We applaud our colleagues from Institut Teknologi Bandung (ITB) for their intelligent conversation throughout the design development. We also express our thanks to colleagues from PT. INKA for supplying the 3D basis model of the crashworthiness structure.

REFERENCES

[1] H. Yang, H. Lei, and G. Lu, “Crashworthiness of circular fiber reinforced plastic tubes filled with composite skeletons/aluminum foam under drop-weight impact loading,” *Thin-Walled Struct.*, vol. 160, p. 107380, Mar. 2021, doi: 10.1016/j.tws.2020.107380.

[2] N. A. Z. Abdullah, M. S. M. Sani, M. S. Salwani, and N. A. Husain, “A review on crashworthiness studies of crash box structure,” *Thin-Walled Struct.*, vol. 153, p. 106795, Aug. 2020, doi: 10.1016/j.tws.2020.106795.

[3] X. Yang, J. Ma, D. Wen, and J. Yang, “Crashworthy design and energy absorption mechanisms for helicopter structures: A systematic literature review,” *Prog. Aerosp. Sci.*, vol. 114, p. 100618, Apr. 2020, doi: 10.1016/j.paerosci.2020.100618.

[4] G. Lu and T. Yu, *Energy Absorption of Structures and Materials*. 2003. doi: 10.1016/j.ijimpeng.2003.12.004.

[5] A. Baroutaji, M. Sajjia, and A. G. Olabi, “On the crashworthiness performance of thin-walled energy absorbers: Recent advances and future developments,” *Thin-Walled Struct.*, vol. 118, no. 1, pp. 137–163, 2017, doi: 10.1016/j.tws.2017.05.018.

[6] H. Molatefi and M. Azizi, “Crashworthiness analysis and energy absorption enhancement of a passenger rail vehicle Crashworthiness Analysis and Energy Absorption Enhancement of a Passenger Rail Vehicle IC255 train and a car in details [7]. Walter studied vehicles and the effects o,” vol. 3, no. December, pp. 45–54, 2016.

[7] R. A. Mayville, K. N. Johnson, R. G. Stringfellow, and D. C. Tyrell, “The development of a rail passenger coach car crush zone,” *Proc. IEEE/ASME Jt. Railr. Conf.*, pp. 55–61, 2003, doi: 10.1115/rtd2003-1653.

[8] S. W. Kirkpatrick, M. Schroeder, and J. W. Simons, "Evaluation of passenger rail vehicle crashworthiness," *Int. J. Crashworthiness*, vol. 6, no. 1, pp. 95–106, 2001, doi: 10.1533/cras.2001.0165.

[9] "The track obstruction by a road vehicle," no. April, 2006.

[10] A. Sutton, "The development of rail vehicle crashworthiness," *Proc. Inst. Mech. Eng. Part F J. Rail Rapid Transit*, vol. 216, no. 2, pp. 97–108, 2002, doi: 10.1243/09544090260082335.

[11] K. Jacobsen, D. Tyrell, and B. Perlman, "Impact test of a crash-energy management passenger rail car," *Am. Soc. Mech. Eng. Rail Transp. Div. RTD*, vol. 27, no. March, pp. 19–26, 2004, doi: 10.1115/RTD2004-66045.

[12] S. Špirk, V. Kemka, M. Kepka, and Z. Malkovský, "Design of a large deformable obstacle for railway crash simulations according to the applicable standard," *Appl. Comput. Mech.*, vol. 6, no. January, pp. 83–92, 2012.

[13] M. Carolan, D. Tyrell, and A. B. Perlman, "Performance Efficiency of a Crash Energy Management System," in *ASME/IEEE 2007 Joint Rail Conference and Internal Combustion Engine Division Spring Technical Conference*, Jan. 2007, pp. 105–115. doi: 10.1115/JRC/ICE2007-40064.

[14] J. Carruthers, C. O. Neill, S. Ingleton, and M. Robinson, "Carruthers J , O ' Neill C , Ingleton S , Robinson M , Grasso M , Roberts J , Prockat J , Simmonds G . The design and prototyping of a lightweight crashworthy rail vehicle driver ' s cab . In : 9th World Congress on Railway Research . 2011 , Lille , Date ," 2015.

[15] K. J. Severson and D. P. Parent, "Train-to-train impact test of crash energy management passenger rail equipment: Occupant experiments," *Am. Soc. Mech. Eng. Rail Transp. Div. RTD*, pp. 1–10, 2006, doi: 10.1115/IMECE2006-14420.

[16] D. Zangani, M. Robinson, and G. Kotsikos, "Improving the Crashworthiness of Aluminium Rail Vehicles," in *Engineering Against Fracture*, Dordrecht: Springer Netherlands, pp. 305–317. doi: 10.1007/978-1-4020-9402-6_24.

[17] X. Xue, F. Schmid, and X. Xue, "Crashworthiness of Conventionally Designed Railway Coaching Stock and Structural Modifications for Enhanced Performance," *5th Eur. LS-DYNA Users Conf.*, vol. 44, no. 1, 2005, [Online]. Available: https://www.dynalook.com/european-conf-2005/copy_of_Xue.pdf

[18] K. Witowski, A. Erhart, P. Schumacher, and H. Müllerschön, "Topology Optimization for Crash," *12th Int. LS-DYNA® Users Conf.*, no. 1, pp. 1–8, 2012.

[19] C. H. Chuang and R. J. Yang, "Benchmark of Topology Optimization Methods for Crashworthiness Design," *12th Int. LS-DYNA® Users Conf.*, no. 2, pp. 1–10, 2012, [Online]. Available: http://www.dynalook.com/international-conf-2012/optimization-metal-forming18-a.pdf

[20] J. Chen, P. Xu, S. Yao, J. Xing, and Z. Hu, "The multi-objective structural optimisation design to improve the crashworthiness of a multi-cell structure for high-speed train," *Int. J. Crashworthiness*, vol. 27, no. 1, pp. 24–33, Jan. 2022, doi: 10.1080/13588265.2020.1773739.

[21] European Comittee for Standardization, *BS EN 15227 - Railway applications - Crashworthiness requirements for railway vehicle bodies*. 2008, p. 38.

[22] B. Halfina, Hendrato, Y.P.D.S. Depari, Muhammad, S.H.M. Kurnia, and H.A. Fitri, "Numerical Analysis for Different Masks of Car Design of High-Speed Train," *Int. J. Automot. Mech. Eng.*, vol. 19, no. 4, pp. 10144–10151, Jan. 2023, doi: 10.15282/ijame.19.4.2022.11.0785.

[23] T. Børvik, A. H. Clausen, M. Eriksson, T. Berstad, O. Sture Hopperstad, and M. Langseth, "Experimental and numerical study on the perforation of AA6005-T6 panels," *Int. J. Impact Eng.*, vol. 32, no. 1–4, pp. 35–64, Dec. 2005, doi: 10.1016/j.ijimpeng.2005.05.001.

[24] Menteri Perhubungan RI, "Standar Spesifikasi Teknis Kereta Kecepatan Normal Dengan Penggerak Sendiri," vol. 2015, pp. 1–32, 2015.

[25] E. Standard, "En 15227," pp. 1–37, 2008.

[26] G. Gao and S. Wang, "Crashworthiness of passenger rail vehicles: a review," *Int. J. Crashworthiness*, vol. 24, no. 6, pp. 664–676, Nov. 2019, doi: 10.1080/13588265.2018.1511233.

[27] X. Xue, R. A. Smith, and F. Schmid, "Analysis of crush behaviours of a rail cab car and structural modifications for improved crashworthiness," *Int. J. Crashworthiness*, vol. 10, no. 2, pp. 125–136, Mar. 2005, doi: 10.1533/ijcr.2005.0332.